

Kohn-Luttinger effect and the instability of a two-dimensional repulsive Fermi liquid at $T=0$

Andrey V. Chubukov*

*Department of Physics and Center for Superconductivity, University of Illinois at Urbana-Champaign,
1110 West Green Street, Urbana, Illinois 61801*

and P. L. Kapitza Institute for Physical Problems, 117973, ul. Kosygina 2, Moscow, Russia

(Received 18 January 1993)

We consider the possibility for a pairing in a two-dimensional (2D) repulsive Fermi liquid due to the singularity in the scattering amplitude $\Gamma(q)$ at the momentum transfer $q \leq 2p_F$ (Kohn-Luttinger effect). A common belief based on perturbative calculations up to second order in the s -wave scattering amplitude is that this effect is absent in two dimensions. I show that this is not the case. For an arbitrary Fermi liquid, $\Gamma(q)$ is found to have a singular part, $\Gamma^{\text{sing}}(q) \sim \sqrt{1 - q^2/(2p_F)^2}$, for $q \leq 2p_F$. For large 2D orbital momentum l , this term gives a dominant *attractive* contribution to the scattering amplitude and leads to a pairing instability in a 2D Fermi liquid with arbitrary short-range repulsion. In the dilute limit, numerical studies show that the effect survives down to $l=1$ and gives rise to a p -wave pairing. The relevance of these results to experiments on ^3He adsorbed on the free surface of ^4He is discussed.

I. INTRODUCTION

The experimental studies of dilute ^3He - ^4He mixture films¹ and multilayers of ^3He adsorbed on graphite,² as well as the search for the new mechanisms of superconductivity in high- T_c materials, renewed the interest to the issue of whether or not the ground state of a two-dimensional (2D) fermionic system with a repulsive interaction is a conventional Fermi liquid. The validity of a Landau-Fermi-liquid description at $T=0$ has recently been questioned by Anderson.³ He argued that the quasiparticle interaction function $f(p, p')$ is singular in 2D for $p \approx p'$ (forward scattering), and this gives rise to a vanishing residue of a quasiparticle Green function at the Fermi surface. Perturbation studies, on the other hand, have found no divergencies which might signal on the breakdown of a Landau-Fermi-liquid description for an arbitrary weak interaction in two dimensions.^{4,5}

The aim of the present study is to consider another possibility for the instability in a 2D repulsive Fermi liquid at $T=0$, this time related to the singularity in the scattering amplitude at zero total momentum $\Gamma(q, -q; q', -q') = \Gamma(q - q')$. The singularity is at the maximum momentum transfer at the Fermi surface $|q - q'| = 2p_F$. It does not break down the Fermi-liquid description of a normal state, but, as we will see, gives rise to an attraction in the scattering amplitude for large angular momentum and, hence, to a pairing instability at sufficiently low T .

In the 3D case, this effect was studied by Kohn and Luttinger⁶ back in 1965. They calculated the leading renormalization of the scattering amplitude in the particle-hole channel (Fig. 1), i.e., the screening of the interaction between quasiparticles at the Fermi surface by the fermionic background, and found the *logarithmical* singularity in $\Gamma(q)$ near $q = |\mathbf{k} - \mathbf{p}| = 2p_F$:

$$\Gamma(q) \sim [(2p_F)^2 - q^2] \ln |(2p_F)^2 - q^2| + \Gamma_{\text{reg}}(q^2),$$

where $\Gamma_{\text{reg}}(q^2)$ is the regular function of a momentum

transfer. The singularity in $\Gamma(q)$ is similar to that for the dielectric constant in a metal.⁷ In a real space, it gives rise to the RKKY-type long-range component of the interaction $\Gamma(r) \sim (1/r^3) \cos(2p_F r + \phi)$. For most of realistic potentials in 3D, this effective long-range interaction decays more slowly than the direct interaction between fermions $U(\mathbf{r} - \mathbf{r}')$. Consequently, it gives dominant contributions to the scattering amplitudes with large angular momentum l , which probe the effective potential at large scales.⁸ The interaction is oscillating in space and a conventional wisdom would be that it may lead to an attraction in Γ_l only for a particular parity of the orbital momentum. This is what one would obtain by simply integrating the singular part of $\Gamma(q)$ at the Fermi surface with the eigenfunctions of the angular momentum, which are the Legendre polynomials in 3D:

$$\Gamma_l = \int \Gamma[q(\theta)] P_n(\cos\theta) \sim (-1)^{l+1} / l^4, \quad q = 2p_F \sin\theta / 2. \quad (1)$$

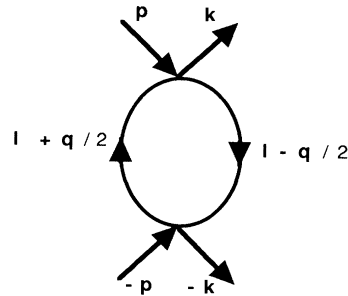


FIG. 1. The diagram of the second order which contributes to the renormalization of the scattering amplitude for the quasiparticles with the opposite momenta at the Fermi surface. For fermions with $S = \frac{1}{2}$, there are four nonequivalent diagrams of the second order. They are shown in Fig. 2.

In fact, however, the factor $(-1)^l$ is absent in Γ_l . The reason is in the spin dependence of the interaction,

$$U(q_1\alpha_1, q_2\alpha_2; q_3\alpha_3, q_4\alpha_4) = U(q_1 - q_3)\delta_{\alpha_1, \alpha_3}\delta_{\alpha_2, \alpha_4},$$

which cannot be neglected for fermions with spin $S = \frac{1}{2}$. Accordingly, one has to sum the contributions to the scattering amplitude from four nonequivalent second-order diagrams in Fig. 2; each of these diagrams has the same schematic form as in Fig. 1.⁹ The simple calculations first done by Kohn and Luttinger⁶ show that, at low density, the contributions from the first three diagrams of Fig. 2 cancel each other while in the fourth, the interaction potential links the momenta \mathbf{k} and $-\mathbf{p}$ rather than \mathbf{k} and \mathbf{p} . Therefore, the effective scattering amplitude, though it has the same functional form as in Eq. (1), is, in fact, a function of the momentum transfer $|\mathbf{k} + \mathbf{p}|$, or alternatively, of $\theta' = \pi - \theta$. Furthermore, the Legendre polynomials obey $P_l(\theta') = (-1)^l P_l(\theta)$ and the integration in Eq. (1) over θ' rather than θ yields

$$\Gamma_l \sim (-1)^l \times (-1)^{l+1} / l^4 \sim (-1) / l^4.$$

We see therefore that the scattering amplitudes with large angular momentum are attractive independently on the parity of l (Ref. 6). The attraction in the scattering amplitudes then gives rise to a pairing instability into a state which corresponds to the most attractive Γ_l .¹⁰

The original approach by Kohn and Luttinger was restricted to the case $l \gg 1$. The extrapolation of the results obtained in this limit to $l=2$, which at that time

was believed to be the angular momentum of the instability in ³He, yielded an extremely small transition temperature $T_c \sim 10^{-40}$. Later, however, the issue was reexamined and it was shown^{11,12} that in the dilute limit the attraction in Γ_l persists down to $l=1$ and $|\Gamma_1|$ is nearly ten times larger than $|\Gamma_2|$. The computed T_c for the p -wave pairing has a reasonable value of $T_c \sim 10^{-3}$ K. Both the value of $T_c^{l=1}$ and particularly its variation in a magnetic field show that this effect is likely to be relevant to the superfluidity in ³He.^{13,14}

In two dimensions, a naive expectation would be that the Kohn-Luttinger effect is even stronger than in the 3D case. However, a simple calculation of the diagram of Fig. 1 for on-site repulsion yields^{13,15}

$$\Gamma(q) = \frac{mU_0^2}{2\pi} \quad (2a)$$

for $q < 2p_F$, and

$$\Gamma(q) = \frac{mU_0^2}{2\pi} \left[1 - \left[1 - \frac{(2p_F)^2}{q^2} \right]^{1/2} \right] \quad (2b)$$

for $q > 2p_F$. As before, $q = |\mathbf{k} - \mathbf{p}|$ and $U_0 = U(k=0)$. We see from Eq. (2b) that there is a square-root singularity in $\Gamma(q)$, which in a real space again gives rise to the long-range component of the effective interaction, $\Gamma(r) \sim \sin 2p_F r / r^2$. However, the singularity in two dimensions is *one sided*: it exists only for a momentum transfer larger than $2p_F$. At the same time, for the particles at the Fermi surface, which are only responsible for a pairing, the effective interaction is given by Eq. (2a) which still has only an s -wave harmonic.

Indeed, the momentum independence of $\Gamma(q)$ for $q < 2p_F$ holds only for a parabolic dispersion of excitations and on-site interaction between quasiparticles. In a general case, the diagram of Fig. 1 may give rise to some momentum dependence of the effective interaction. This is a way how one can study pairing instabilities in the low-density 2D Hubbard model.¹⁶ However, for arbitrary short-range repulsion, $\Gamma(q)$ inferred from the diagram in Fig. 1 remains an *analytic* function of a momentum transfer for all $q < 2p_F$. Therefore, at this stage of consideration, no model-independent statement can be made about pairing instability in a 2D Fermi liquid.¹⁷

The aim of the present paper is to show that the Kohn-Luttinger singularity in $\Gamma(q)$ in fact exists on both sides of $q = 2p_F$, even for a parabolic dispersion of excitations and on-site repulsion. However, to find the singularity at $q < 2p_F$, one has to go beyond the second order in the perturbation theory (Secs. II A and II B). Furthermore, the singularity unambiguously leads to an *attraction* in the scattering amplitude for large angular momentum (Sec. II C). In the dilute limit, the attraction in the scattering amplitudes persists down to $l=1$ and the p -wave component is the most attractive (Sec. II D). Finally, we show that the singularity in $\Gamma(q)$ is a Fermi-liquid effect—it exists in arbitrary dense Fermi liquid (Sec. II E). We also discuss the relevance of our results to the experiments on ³He adsorbed on the free surface of ⁴He.

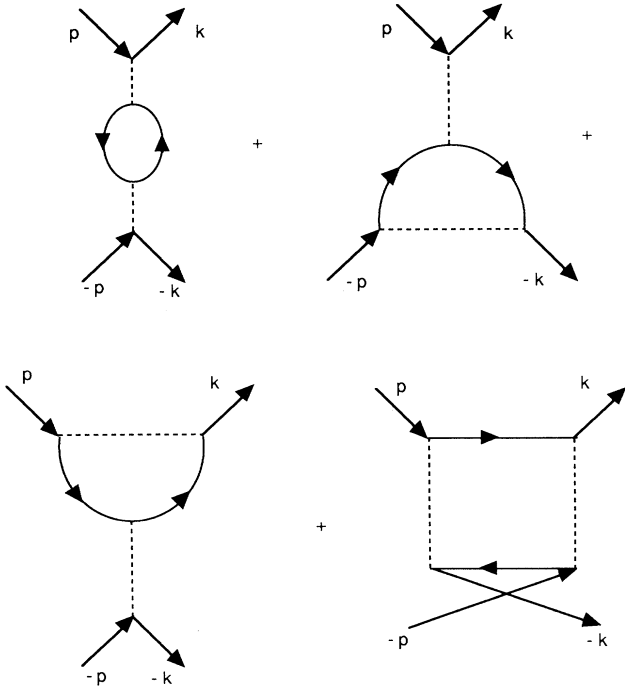


FIG. 2. The diagrams which contribute to the renormalization of the scattering amplitude for fermions with $S = \frac{1}{2}$. Each of these diagrams has the same schematic form as in Fig. 1.

II. KOHN-LUTTINGER EFFECT IN 2D

A. Physical origin for the effect

To clarify the physical origin for the effect consider the simplest case of a Fermi gas of particles with a parabolic dispersion: $\epsilon_k = (p^2 - p_F^2)/2m$. We neglect for a moment the spin dependence of the interaction and focus again on the particle-hole bubble of Fig. 1. Clearly, the fermions inside the bubble should be on the opposite sides of the Fermi surface. We consider the situation when the external particles are at the Fermi surface, i.e., $q < 2p_F$. In this case, the restrictions imposed by the frequency integration restrict the integration over the intermediate momenta l to the region $l_2 < l < l_1$, where

$$l_{1,2} = \pm \frac{q \cos\phi}{2} + \frac{q}{2} \sqrt{\epsilon^2 + \cos^2\phi},$$

$$\epsilon^2 = [(2p_F)^2 - q^2]/q^2, \quad (3)$$

and ϕ measures the direction of l with respect to q (we have chosen $\cos\phi > 0$). A simple calculation then gives

$$\Gamma(q) = \frac{m}{2\pi^2 q} \int_{-\pi/2}^{\pi/2} \frac{d\phi}{\cos\phi} \int_{l_2}^{l_1} dl \Phi_+ \Phi_- . \quad (4)$$

Here Φ_{\pm} are the vertex functions which depend on $t_{\pm} = l \pm (\mathbf{k} + \mathbf{p})/2$ and, in general, on $\Omega_{\pm} \sim [l \pm (\mathbf{k} + \mathbf{p})/2]^2 - p_F^2$. In the absence of a renormalization, Φ_{\pm} coincide with the interaction potential, which is a *regular* function of t_{\pm}^2 . It then immediately follows that $\Gamma(q)$ at the Fermi surface is free from singularities simply because $l_1 - l_2 = q \cos\phi$ and the dangerous $\cos\phi$ factor in the denominator in Eq. (4) is canceled out. In fact, with some more efforts one can prove that the regular behavior of $\Gamma(q)$ holds for arbitrary dispersion of excitations.¹⁶ We show, however, that it does not survive the effect of vertex corrections. To see how this happens, we first recall that in 3D, the logarithmical singularity in $\Gamma(q)$ comes from the region of l , where both $|l|$ and $\cos\phi$ are of the order of ϵ . Let us consider the contribution to $\Gamma(q)$ from the same region in the 2D problem. When $\epsilon \ll 1$, $q = |(\mathbf{k} - \mathbf{p})/2| \approx 2p_F$ and $|(\mathbf{k} + \mathbf{p})/2| = O(\epsilon)$. Hence, in the region which we selected, the total incoming momentum for Φ_{\pm} is nearly zero: $t_{\pm} = O(\epsilon)$, and the total frequencies are even far smaller: $|\Omega_{\pm}| = O(\epsilon^2)$. In this situation, the renormalization of Φ_{\pm} in the Cooper channel necessarily produces the term $\ln t_{\pm}^2/p_F^2$, which is *singular* in t_{\pm}^2 and in case of attraction would lead to the conventional pairing instability. For the present purposes, the divergence of this term at $t_{\pm} \rightarrow 0$ is not by itself crucial because the renormalized vertex should be substituted into the particle-hole channel and integrated over the intermediate momenta t_{\pm} . However, the logarithm gives rise to the nonanalyticity in Φ_{\pm} such that the expansion of Φ_{\pm} over ϵ^2 holds in ϵ^2/t_{\pm}^2 and breaks down when t_{\pm} , and hence the internal momentum in the particle-hole bubble, l , is of the order of ϵ . As a result, upon substituting the logarithmical term into the particle-hole bubble and integrating over momentum, we obtain the contribution to $\Gamma(q) - \Gamma(2p_F)$, which by a simple power counting should be of the form

$I \sim \epsilon^2 \int \int d\phi dl / l^2 \cos\phi$, where the lower limit in each integration is of the order of ϵ . Further, the integration in I is confined to the region where l and $\cos\phi = O(\epsilon)$, which, in turn, justifies the selection made above, and yields $I \sim \epsilon$. Therefore,

$$\Gamma(q) - \Gamma(2p_F) \sim \epsilon \sim \sqrt{1 - q^2/(2p_F)^2},$$

which implies that square-root singularity in $\Gamma(q)$ is present for the momentum transfer at the Fermi surface as well.

B. Dilute limit

It is instructive to begin the quantitative treatment with the dilute limit $r_0 p_F \ll 1$, where r_0 is the range of the potential. In this limit, one can perform the perturbative expansion in the s -wave scattering amplitude f_0 , which is a dimensionless quantity in two dimensions.¹⁰ It was several times in the literature^{18,13,15} that the 2D density of states at the Fermi surface does not depend on p_F and the expansion parameter thus does not coincide with $r_0 p_F$, even if the Born parameter is of the order of unity. In fact, the smallness of the s -wave scattering amplitude f_0 in the dilute limit in 2D, which justifies the perturbative expansion at low densities, is related only to the logarithmical singularity of the vertex renormalization for the two particles in a vacuum. This renormalization holds in a particle-particle channel and transforms the interaction potential into the scattering amplitude which accounts for all scattering processes for two isolated particles. In three dimensions, this renormalization is not crucial, and at least when the Born parameter is small, the total s -wave scattering amplitude is not very different from the bare one ($= mU_0/4\pi$ where U_0 is the zeroth Fourier component of the potential). In two dimensions, the two-particle vertex renormalization is more significant, and for small U_0 , the ladder summation in the particle-particle channel changes the bare amplitude to

$$f_0 = \frac{mU_0/4\pi}{1 + (mU_0/4\pi) \ln(r_0 p_F)^{-2}} . \quad (5)$$

It is convenient to reexpress f_0 as $f_0 = -1/2 \ln ap_F$, where a is the effective s -wave scattering length. Then, for weak interaction, we have $a = r_0 \exp -2\pi/mU_0$. For most of realistic potentials in 2D, however, the Born parameter ($= mU_0/4\pi$ in two dimensions) is of order of unity and a is likely to be of the same order as r_0 . In any event, for small enough ap_F , the total scattering amplitude is a small number, which validates the perturbative expansion at low density.

Furthermore, at low density, it is sufficient to consider only the first corrections to the particle-hole bubble of Fig. 1. The relevant diagrams of the third order in f_0 are schematically shown in Fig. 3. From the earlier discussion we expect the most singular diagram to have vertex renormalization in the particle-particle channel as in Fig. 3(a). In fact, for $S = \frac{1}{2}$ fermions, we again have four non-equivalent diagrams of this kind (Fig. 4). In the dilute limit, the difference between $U(0)$ and $U(2p_F)$ is negligible and the summation over spin indices of virtual fer-

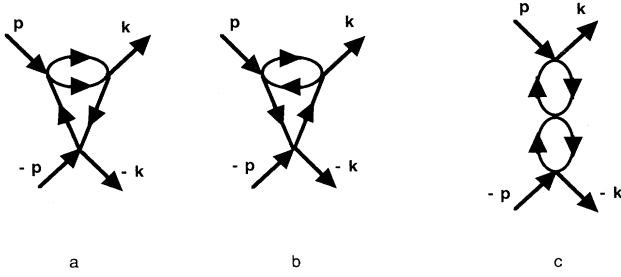


FIG. 3. The third-order diagrams for the renormalization of the scattering amplitude $\Gamma(q)$. The spin indices are omitted, as in Fig. 1. The singularity in $\Gamma(q)$ at the momentum transfer $q = |\mathbf{k} - \mathbf{p}| \leq 2p_F$ is chiefly due to the first diagram where the vertex renormalization is in the particle-particle channel. One-half of all diagrams is presented. The second half describes the renormalization of the lower vertex in Fig. 1.

mions leads to the same result as for the second-order diagrams; namely, the contributions from the first three diagrams in Fig. 4 cancel each other and only the fourth diagram, where the relative momentum in the particle-hole bubble is $\mathbf{q}' = \mathbf{k} + \mathbf{p}$, contributes to the effective scattering amplitude. To simplify the discussion of how the calculations were carried out, we continue to refer to the schematic diagram of Fig. 3 but keep in mind that the scattering amplitude is, in fact, a function of \mathbf{q}' and therefore the result for Γ_l which we will soon obtain, should be multiplied by an extra factor of $(-1)^l$.

In evaluating the diagram of Fig. 3(a), we first integrate

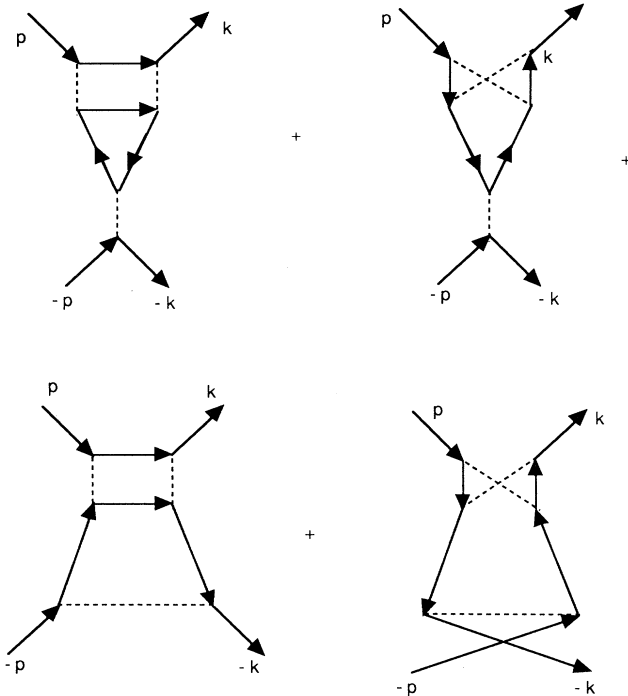


FIG. 4. Nonequivalent diagrams for fermions with $S = \frac{1}{2}$ which have the same schematic form as the diagram in Fig. 3(a).

over the intermediate frequency and momenta in the Cooper channel. Clearly, the frequency integration yields a nonzero result only if both intermediate fermions are either above or below the Fermi surface. The integration over frequency is straightforward and yields vertex renormalization in the form

$$\Phi_{\pm} = U_0 \left[1 + \frac{mU_0}{4\pi} \lambda_{\pm} \right], \quad (6)$$

where

$$\lambda_{\pm} = -2 \ln r_0 p_F - \ln t_{\pm}^2 / p_F^2 + \lambda_{\pm}^{\text{reg}}. \quad (7)$$

Here, as before, $\mathbf{t}_{\pm} = \mathbf{1} \pm (\mathbf{k} + \mathbf{p})/2$. Also, $2l$ is the total momentum in the particle-hole bubble, and $\lambda_{\pm}^{\text{reg}}$ is a contribution to the renormalized vertex which does not diverge when either $p_F \rightarrow 0$ or $t_{\pm} \rightarrow 0$. A substitution of the regular part of Φ_{+} into the particle-hole channel does not give rise to a nonanalyticity in $\Gamma(q)$, and we neglect $\lambda_{\pm}^{\text{reg}}$ below.

The first term in Eq. (7) is parametrically large at low densities. However, it does not contain any dependence on the transferred momenta and therefore is irrelevant for the Kohn-Luttinger effect. Moreover, this term can easily be recognized as the first term in the ladder series which transforms the interaction potential for two particles in a vacuum into the scattering amplitude f_0 [Eq. (5)]. We emphasize its dependence on r_0 , which serves as the upper cutoff in the momentum integration. The $\ln r_0 p_F$ contribution thus comes from the region in the momentum space which is located relatively far from the Fermi surface. On the other hand, the second logarithmical term in Eq. (7) is the same as in the conventional Cooper problem and is due to the integration over momenta in the immediate vicinity of the Fermi surface. We therefore can separate the momentum integration in the particle-particle channel into the integral over the immediate vicinity of the Fermi surface and the integral over the regions away from the Fermi surface. In the second integral, $\ln r_0 p_F$ is the dominant term, and the vertex renormalization is the same as for two isolated particles with $p = p_F$ and $\epsilon_p = p^2/2m$. Consequently, the integration away from the Fermi surface transforms the interaction potential U_0 into $4\pi f_0/m$, which then can be regarded as the effective vertex for the momentum integration near the Fermi surface. Accordingly, we rewrite the expression for Φ_{\pm} as

$$\Phi_{\pm} = \frac{4\pi f_0}{m} [1 + f_0 \ln p_F^2 / t_{\pm}^2]. \quad (8)$$

We now substitute (8) into the particle-hole bubble and integrate over the intermediate frequency and momentum. The frequency integration can be done exactly and for q slightly less than $2p_F$ we obtain

$$\Gamma(q) = \frac{8f_0^3}{m} \int_0^{\pi/2} \frac{d\phi}{\cos\phi} \int_{\bar{l}_1}^{\bar{l}_2} d\bar{l} \ln[(\epsilon^2 - \bar{l}^2)^2 + 4\epsilon^2 \bar{l}^2 \cos^2\phi], \quad (9)$$

where $\bar{l}_{1,2} = l_{1,2}/q = \pm \cos\phi/2 + \frac{1}{2}\sqrt{\epsilon^2 + \cos^2\phi}$, and as be-

fore, $\epsilon^2 = [(2p_F)^2 - q^2]/q^2 \ll 1$. Next, we discussed in the previous section that the nonanalytical contribution to $\Gamma(q)$ is confined to the region in the momentum space where $\cos\phi = O(\epsilon)$ and hence $\bar{l}_{1,2} = O(\epsilon)$. In this region, the dependence on ϕ in the logarithm can be neglected and the integration over \bar{l} can be done analytically. Introducing $\pi/2 - \phi = \epsilon z$ and carrying out the integration over \bar{l} , we obtain

$$\Gamma(q) = \Gamma(2p_F) + \frac{32f_0^3}{m} \epsilon \int_0^\beta \frac{dz}{z} \Pi_z. \quad (10)$$

Here

$$\Pi_z = \sqrt{z^2 + 1} \ln[z + \sqrt{z^2 + 1}] - z \ln 2z.$$

The upper cutoff in the integral over z is not specified precisely, we only know that $\beta = O(1/\epsilon)$. However, a simple inspection of (10) shows that at large z , $\Pi_z \sim (2z)^{-1} \ln 2z$. The integral in (10) is therefore convergent at the upper cutoff and we can set $\beta = \infty$. The subsequent integration can be done exactly and we obtain

$$\begin{aligned} \Gamma(q) &= \Gamma(2p_F) + \Gamma^{\text{sing}}(q); \\ \Gamma^{\text{sing}}(q) &= f_0^3 \frac{8\pi^2}{m} \left[1 - \frac{q^2}{(2p_F)^2} \right]^{1/2}. \end{aligned} \quad (11)$$

It clearly follows from (11) that the singularity in $\Gamma(q)$ indeed exists not only for $q > 2p_F$, as in Eq. (2a), but also for the momentum transfer at the Fermi surface, where $q < 2p_F$. We now proceed to the pairing problem.

C. Pairing problem

Equation (11) defines the effective interaction between two particles at the Fermi surface with zero total momentum. This is indeed the irreducible vertex for the Cooper problem. To solve the Cooper problem, we now have to expand the interaction in the eigenfunctions of the angular momentum.¹⁰ Under this procedure, the integral equation for the total pairing vertex $\bar{\Gamma}$ decouples to a set of algebraic equations for its partial components $\bar{\Gamma}_l$. In each equation, a partial component of the total vertex is coupled to a partial component of the irreducible vertex with the same angular momentum:¹⁰

$$\bar{\Gamma}_l = \frac{\Gamma_l}{(1 + \Gamma_l \Pi)}. \quad (12)$$

Here $\Pi \sim \ln \epsilon_F / T$ is the polarization operator for the particles at the Fermi surface. The decoupling in the Cooper channel has a very strong consequence—we see that the Fermi-liquid state at $T=0$ is unstable against pairing if there is an attraction even for a single Γ_l .

In two dimensions, the normalized eigenfunctions for the angular momentum are

$$\Phi_l = \sqrt{2} \cos l\theta \left[\frac{1}{\pi} \int_0^\pi \Phi_l^2 d\theta = 1 \right]. \quad (13)$$

The angular variable θ is related to q as $q = 2p_F \sin(\theta/2)$. For large l , Γ_l probes the interaction at large distances where the contribution from the singular part of $\Gamma(q)$ is dominant. Integrating $\Gamma^{\text{sing}}(q)$ from Eq. (11) with the

eigenfunctions Φ_l and recalling that we have to multiply the answer by $(-1)^l$ because only the fourth diagram in Fig. 4 actually contributes to $\Gamma(q)$, we obtain

$$\Gamma_l = -\frac{8\pi f_0^3}{\sqrt{2}m} \frac{1}{l^2}. \quad (14)$$

We see that the scattering amplitudes with large angular momentum are *attractive* independently on the form of the short-range interaction potential in two dimensions. Solving further a conventional weak-coupling Cooper problem we finally obtain $T_c^l \sim \exp -1/|g_l|$, where

$$g_l = -2f_0^3/l^2. \quad (15)$$

We now have to justify the restriction with only the first diagram in Fig. 3. There are two other diagrams of the third order. The diagram of Fig. 3(c) is simply the next term in the RPA series for the polarization operator. In the absence of a singular behavior of a pure particle-hole bubble, it does not give rise to any singularity in $\Gamma(q)$ for $q < 2p_F$. The diagram of Fig. 3(b) has the same structure as that of Fig. 3(a), but the renormalization of Φ_\pm is now in the particle-hole channel. The external momenta for Φ_\pm are $|t_\pm| < 2p_F$ and hence the renormalized vertex acquires some momentum dependence only due to a finite external frequency Ω_\pm . In essence, the momentum-dependent term in the renormalized vertex in Fig. 3(b) has an extra factor of Ω_\pm/t_\pm compared to that in Eq. (7). Earlier we found that the singular contribution to $\Gamma(q)$ is confined to the region where $l = O(\epsilon)$ and $\cos\phi = O(\epsilon)$. In this region,

$$\Omega_\pm = \left[1 \pm \frac{\mathbf{k} \cdot \mathbf{p}}{2} \right]^2 - p_F^2 = O(\epsilon^2),$$

while $t_\pm = O(\epsilon)$. Hence, $\Omega_\pm/t_\pm \sim O(\epsilon) \ll 1$ and the diagram of Fig. 3(b) should be less singular than the diagram of Fig. 3(a). This is indeed what we obtained by carrying out the calculations explicitly. We found that the diagram in Fig. 3(b) has only a logarithmical singularity at $\epsilon \rightarrow 0$:

$$\Gamma_{3b}^{\text{sing}}(q) \sim \frac{f_0^3}{m} \ln \left[1 - \frac{q^2}{(2p_F)^2} \right]. \quad (16)$$

The integration with the eigenfunctions of angular momenta then yields $\Gamma_l \sim l^{-3}$ which for $l \gg 1$ is much smaller than $\Gamma_l \sim l^{-2}$, which we obtained for the diagram of Fig. 3(a).

D. *p*-wave pairing in the dilute limit

The preceding discussion was focused on the case of large angular momenta, where the attraction in $\Gamma(q)$ is directly related to the long-range component of the effective interaction between quasiparticles. In this case, we could only conclude that the instability is indeed present, but the value of l , which corresponds to the most attractive Γ_l remained undecided. In fact, at low density, there is no need to expand in both f_0 and l . We certainly may restrict the description to an expansion in f_0 only

and solve the problem exactly for all l . We first note that as l decreases from the initially large value, the contribution from $\Gamma^{\text{sing}}(q)$ in Eq. (11) grows by the absolute magnitude but at the same time, the repulsive contribution from the regular part of $\Gamma(q)$ also becomes more competitive. A balance between these two effects gives rise to a maximum in $|\Gamma_l|$ at some value of l . We further note that because Γ_l in (15) grows rather rapidly (as $1/l^2$), the small values of l ($l=1, 2, \dots$) are of special interest. For small l , analytical consideration is difficult to carry out, but the numerical evaluation of the diagrams is straightforward. We found that the diagrams of Figs. 3(a) and 3(b) are equally important at small l , and computing the integrals obtained:

$$g_1 = -4.1 \times f_0^3, \quad g_2 = 0.11 \times g_1, \quad \dots \quad (17)$$

For $l > 2$, g_l are well approximated by the asymptotic expression of Eq. (15). We see that the attraction in Γ_l survives down to $l=1$ and g_1 is the largest among $|g_l|$. We thus conclude that a dilute two-dimensional Fermi gas with repulsive interaction is unstable with respect to a p -wave pairing, much like it happens in three dimensions, where¹¹

$$g_1^{3D} = -\frac{4(2 \ln 2 - 1)}{5\pi^2} (f_0^{3D})^2 \approx -0.031 (f_0^{3D})^2,$$

$$f_0^{3D} = ap_F.$$

Note that while the coupling constant in 2D has one extra power of the s -wave scattering amplitude in comparison with that in the 3D case, the numerical coefficient in Eq. (17) is far larger than in g_1^{3D} .

E. Dense Fermi liquid

The above discussion was restricted to the dilute limit. In fact, as Kohn and Luttinger have shown for the 3D case,⁶ the singularity in $\Gamma(q)$ is related only to the sharpness of the Fermi surface and therefore should exist in an arbitrary dense Fermi liquid. In this section we show that the same is also true for a 2D Fermi liquid. Specifically, we show that the singularity in $\Gamma(q)$ is related to the momentum and frequency integration only in the immediate vicinity of the Fermi surface where quasi-particle excitations are well defined at arbitrary density, and the Green function has the form

$$G(\mathbf{k}, \omega) = \frac{Z}{\omega - \epsilon_k + i\delta \text{sgn}\omega}, \quad (18)$$

where $\epsilon_k = v_F(p - p_F)$. To see this, consider the total irreducible vertex for the Cooper channel (Fig. 5). In analogy with the perturbative expansion, we select the particle-hole bubble, where the integration is confined to the particular region near the Fermi surface, where the total momentum in the bubble is small ($\sim \epsilon$) and nearly orthogonal to the relative momentum $\mathbf{q} = \mathbf{k} - \mathbf{p}$. The shaded vertices in Fig. 5 then represent the total scattering amplitudes $\bar{\Phi}_{t_{\pm}} = \bar{\Phi}_{t_{\pm}}(q)$ for the particles with small total momentum $t_{\pm} = O(\epsilon)$ (we keep the same notations as at low density). For $t_{\pm} \ll p_F$, the leading contribution

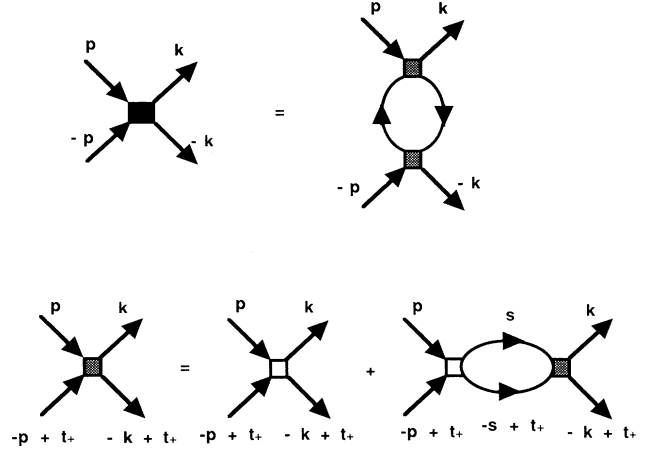


FIG. 5. The diagrams which contribute to the irreducible bare vertex for the Cooper channel in a dense 2D Fermi liquid at $q \leq 2p_F$. We select the particle-hole bubble, where the integration is confined to the region in the momentum space, where the total momentum in the bubble is small and nearly orthogonal to $\mathbf{p} - \mathbf{k}$. In this region, each of the shaded vertices has nearly zero total momentum (see text) and the dominant vertex renormalization is in the particle-particle channel. The spin indices are omitted for simplicity and can be restored in the same way as in Fig. 4.

to $\bar{\Phi}_{t_{\pm}}$ comes from the particle-particle channel where the polarization operator has the logarithmical Cooper-like term $\sim \ln t_{\pm}/p_F$. We emphasize that it also comes from the momentum integration right near the Fermi surface. Accordingly, we represent each of the vertices as a sum of ladder diagrams (Fig. 5). The irreducible vertex in this series, $\bar{\Phi}_{t_{\pm}}^0$, now includes all nonsingular contributions from the particle-hole and particle-particle channels and is some unknown function of the momentum transfer q . To find $\bar{\Phi}_{t_{\pm}}$, we expand $\bar{\Phi}$ and $\bar{\Phi}^0$ in the series of the eigenfunctions of the angular momenta \bar{l} and solve the problem independently for each \bar{l} . The solutions for different \bar{l} differ by numerical factors, but the leading logarithmical dependence on t_{\pm} is the same for all \bar{l} . For a repulsive interaction we then obtain:

$$\bar{\Phi}_{\bar{l}} = \frac{\alpha_{\bar{l}}}{Z^2 m^* \ln p_F / t_{\pm}},$$

where $m^* = p_F/v_F$ is the effective mass of a quasiparticle and $\alpha_{\bar{l}}$ is an unknown numerical factor, which depends on l . The total vertex function is then given by

$$\bar{\Phi}_{t_{\pm}}^t(q) = \frac{A(q)}{Z^2 m^* \ln p_F / t_{\pm}}, \quad (19)$$

where $A(q)$ is some regular dimensionless function of q , whose partial components are α_l . We then substitute the renormalized vertices into the particle-hole bubble and integrate over small t_{\pm} . The integration proceeds along the same lines as in the dilute case, and we obtain:

$$\Gamma(q) = \frac{8\pi^2 B(q)}{m^* Z^2} \frac{\epsilon}{\ln^3 1/\epsilon} \left[1 + O\left(\frac{1}{\ln \epsilon}\right) \right] + \Gamma^{\text{reg}}(q^2). \quad (20)$$

Here $B(q)$ is the product of the two A functions. It is not, however, simply equal to $A^2(2p_F)$ because once again we have to be careful about the spin dependence of the interaction. We already discussed in Sec II B that, in fact, there are four nonequivalent diagrams with the same structure as in Fig. 5 (see Fig. 4). They all contribute to $\Gamma(q)$ and, carrying out the summation over spin indices, we obtain the following expression for the scattering amplitudes with large angular momentum l :

$$\Gamma_l = -\frac{8\pi^2}{m^* Z^2} \bar{B}_l \frac{1}{\sqrt{2} l^2 \ln^3 l} \left[1 + O\left(\frac{1}{\ln l}\right) \right], \quad (21)$$

where

$$\bar{B}_l = A^2(0) + 2(-1)^l [A(0)A(2p_F) - A^2(2p_F)]. \quad (22)$$

Note that \bar{B}_l looks much like its analog in the 3D case.⁶ We see that for large l , Γ_l are *negative*, at least for odd l , no matter what the form of $A(q)$ is. A solution of the Cooper problem then yields $T_c^l \sim \exp -1/|g_l|$, where

$$g_l = -2\bar{B}_l \frac{1}{l^2 \ln^3 l}. \quad (23)$$

The actual transition is clearly into a state which corresponds to the most attractive Γ_l . It is striking that Eq. (23) contains neither the effective mass nor the residue of the quasiparticle Green function.

Indeed, Eq. (23) is the asymptotic expression which, strictly speaking, is valid only when $\ln l \gg 1$. At the same time, the attraction in Γ_l in this limit is the *universal* feature of a Fermi liquid which does not depend on the details of the interaction between quasiparticles, as long as the interaction is short ranged.

III. CONCLUSION

In this paper, we discuss the possibility for a pairing in a repulsive 2D Fermi liquid due to the singularity in the scattering amplitude at the momentum transfer $q \leq 2p_F$ (Kohn-Luttinger effect). This effect was believed to be absent in two dimensions because the leading renormalization of the interaction potential in the dilute limit does not give rise to any singularity in the scattering amplitude for a momentum transfer at the Fermi surface (i.e., for $q < 2p_F$). We have shown that the absence of the effect is an artifact of restricting with only the leading order in the perturbation expansion. We performed calculations beyond the leading order and found that the scattering amplitude $\Gamma(q)$ for the particles at the Fermi surface, in fact, has the square-root singularity for a momentum transfer less than $2p_F$. In the dilute limit, the

singularity in $\Gamma(q)$ leads to an attraction in the scattering amplitudes with large angular momentum independently on the parity of l . Furthermore, we found that the attraction in Γ_l persists down to $l=1$ and Γ_1 is the most attractive component. Therefore, a dilute two-dimensional Fermi gas with repulsive interaction is unstable with respect to the p -wave pairing, much like it happens in three dimensions. Finally, we have shown that the singularity in $\Gamma(q)$ at the Fermi surface exists in an arbitrary dense Fermi liquid and gives rise to a pairing instability no matter what the form is of a short-range interaction potential.

The results obtained here are likely to be applied to dilute ^3He - ^4He mixture films. At low temperatures, ^3He is known^{19,1} to be bound at the surface of ^4He with an energy of 2.2 K. The adsorbed atoms are free to move along nearly equipotential surface of ^4He and form a 2D Fermi liquid. This “surface” ^3He survives up to about the densities in the atomic layer of pure liquid ^3He .

The early studies of surface tension²⁰ and the velocity of surface sound²¹ were fitted to the 2D Fermi-liquid theory with a momentum-independent interaction potential¹ and have led to a *positive*, but rather small, scattering amplitude $f_0 \sim 0.1$ for coverages of ^3He up to $x=0.3$ ($x=1$ corresponds to the areal density in the atomic layer of pure ^3He). We fitted the more recent NMR susceptibility data²² to a weak-coupling Landau-Fermi-liquid theory¹⁸ and obtained $f_0 \sim 0.3$ for $x=0.65$, the largest coverage before a steplike doubling of magnetization occurs. For this value of f_0 , $T_c^{l=1} \sim 10^{-4}$ K. On the other hand, the data of the specific-heat measurements²³ were interpreted as evidence that the “surface” ^3He condenses into a high-density phase, and the area occupied by the dense ^3He increases with x . If this is the case, then one may expect to find larger values of f_0 and hence a much higher $T_c^{l=1}$. However, the conclusion about p -wave pairing was, strictly speaking, restricted to low densities. At high densities of ^3He , the momentum dependence of the interaction potential and the deviation of the quasiparticle spectrum from the parabolic form should also be considered in the calculations of $T_c^{l=1}$. The quantitative study of these effects in “surface” ^3He have yet been done.

ACKNOWLEDGMENTS

I am grateful to G. Kotliar for the discussions which stimulated the present work. It is my pleasure to also thank J. R. Engelbrecht, D. Frenkel, L. P. Gorkov, A. Meyerovich, A. Sokol, S. Sachdev, R. Shankar, and P. Wiegmann for stimulating conversations. The work was supported by NSF Grant No. DMR 88-09854 through the Science and Technology Center for Superconductivity at the University of Illinois at Urbana-Champaign. I am also thankful to the Aspen Center for Physics, where this work was completed.

*Present address: Department of Physics, Yale University, 217 Prospect Street, New Haven, Connecticut 06511-8167.

¹D. O. Edwards and W. F. Saam, in *Progress in Low Temperature Physics*, edited by D. F. Brewer (North-Holland, Amsterdam,

1978), Vol. 7a, p. 282.

²D. S. Greywall, *Phys. Rev B* **41**, 1842 (1990).

³P. W. Anderson, *Phys. Rev. Lett.* **65**, 2306 (1990); **66**, 3226 (1991); see also P. C. E. Stamp, *ibid.* **68**, 2180 (1992).

- ⁴P. Bloom, Phys. Rev. B **12**, 125 (1975).
- ⁵J. R. Engelbrecht and M. Randeria, Phys. Rev. Lett. **65**, 1032 (1990); H. Fukuyama, Y. Hasegawa, and O. Narikiyo, J. Phys. Soc. Jpn. **60**, 2013 (1991).
- ⁶W. Kohn and J. H. Luttinger, Phys. Rev. Lett. **15**, 524 (1965).
- ⁷H. Friedel, Adv. Phys. **3**, 446 (1954); W. Kohn, Phys. Rev. Lett. **2**, 393 (1959).
- ⁸L. P. Pitaevskii, Zh. Eksp. Teor. Fiz. **37**, 1794 (1960) [Sov. Phys. JETP **10**, 1267 (1960)]; L. P. Gorkov and L. P. Pitaevskii, *ibid.* **42**, 600 (1962) [*ibid.* **15**, 417 (1962)].
- ⁹The Kohn-Luttinger effect for spinless fermions was considered in, R. Shankar, Physica A **177**, 530 (1991).
- ¹⁰E. M. Lifshitz and L. P. Pitaevskii, *Statistical Physics* (Pergamon, New York, 1980), Part 2.
- ¹¹D. Fay and A. Layzer, Phys. Rev. Lett. **20**, 187 (1968).
- ¹²M. Yu. Kagan and A. V. Chubukov, Pis'ma Zh. Eksp. Teor. Fiz. **47**, 525 (1988) [JETP Lett. **47**, 614 (1988)].
- ¹³M. A. Baranov, A. V. Chubukov, and M. Yu. Kagan, Int. J. Mod. Phys. B **6**, 2471 (1992).
- ¹⁴P. G. van de Haar, G. Frossati, and K. S. Bedell, J. Low Temp. Phys. **77**, 35 (1989); G. Frossati, S. A. Wieggers, T. Hata, R. Jochemsen, P. G. van de Haar, and L. P. Roobol, Chekh. J. Phys. B **40**, 909 (1990); U. E. Israelson, B. C. Crooker, H. M. Bolzer, and C. M. Gould, Phys. Rev. Lett. **53**, 1943 (1984).
- ¹⁵A. M. Afanas'ev and Yu. Kagan, Zh. Eksp. Teor. Fiz. **42**, 1456 (1962) [Sov. Phys. JETP **15**, 1009 (1962)].
- ¹⁶M. A. Baranov and M. Yu. Kagan, Z. Phys. B **86**, 237 (1992); A. V. Chubukov and J. P. Lu, Phys. Rev. B **46**, 11 163 (1992).
- ¹⁷M. A. Baranov and M. Yu. Kagan, Zh. Eksp. Teor. Fiz. **99**, 1236 (1991) [Sov. Phys. JETP **72**, 689 (1991)].
- ¹⁸J. R. Engelbrecht, M. Randeria, and L. Zhang, Phys. Rev. B **45**, 10 135 (1992).
- ¹⁹A. F. Andreev, Zh. Eksp. Teor. Fiz. **50**, 1415 (1966).
- ²⁰K. N. Zinov'eva and S. T. Boldarev, Zh. Eksp. Teor. Fiz. **56**, 1089 (1969) [Sov. Phys. JETP **29**, 585 (1969)].
- ²¹D. O. Edwards, S. Y. Shen, J. R. Eskardt, P. P. Fatouros, and F. M. Gasparini, Phys. Rev. B **12**, 892 (1975).
- ²²J. M. Valles, Jr., R. H. Higley, R. B. Johnson, and R. B. Hallock, Phys. Rev. Lett. **60**, 428 (1988); R. H. Higley, D. T. Sprague, and R. B. Hallock, *ibid.* **63**, 2570 (1989).
- ²³B. K. Bhattacharyya and F. M. Gasparini, Phys. Rev. B **31**, 2719 (1985).